ISSN 1870-4069

# Automatic Image-based Galaxy Classification: An Approach Using Fractal Dimension Analysis

Jorge de la Calleja[1], Elsa de la Calleja[2], Hugo Jair Escalante[3], Eduardo López-Domínguez[4], María Auxilio Medina-Nieto[1], Marco Aurelio Nuño-Maganda[5]

[1] Universidad Politécnica de Puebla, Mexico

[2] Universidad Nacional Autónoma de México, Instituto de Investigaciones en Materiales, Mexico

[3] Instituto Nacional de Astrofísica, Óptica y Electrónica, Computer Science Department, Puebla, Mexico

[4] National Polytechnic Institute, Department of Computer Science, Center for Research and Advanced Studies, Mexico

[5] Universidad Politécnica de Victoria, Tamaulipas, Mexico

jorge.delacalleja@uppuebla.edu.mx, elsama79@gmail.com, hugojair@inaoep.mx, eduardo.lopez.dom@cinvestav.mx, mnunom@upv.edu.mx

**Abstract.** The fractal dimension is a measure of complexity which provides structural and spatial information of an object. This physical measurement has been used in the evaluation of several structural properties of the objects and phenomena of the Universe. The Universe contains billions of galaxies, which are large systems of stars and cloud of gases; galaxy classification permits to understand the origin and evolution of the Universe. In this work we present an experimental study for image-based galaxy classification using features extracted with principal component analysis, and combining them with the measure of *Haussdorf-Besicovich* fractal dimension. The classification stage was performed using well-known machine learning algorithms: C4.5, k-nearest neighbors, random forest and support vector machines; considering the three main types of galaxies: elliptical, spiral and irregular. Experimental results using 10-fold cross-validation show that the fractal dimension value allows to improve the galaxy classification yielding an accuracy of 86.71% using the random forest classifier.

**Keywords:** Fractal dimension, machine learning, galaxy classification.

## 1 Introduction

Astronomy has a long history of acquiring and analyzing enormous quantities of data. As many other fields, this science has become very data-rich due to advances in telescope, detector, and computer technology. Recently, numerous digital sky surveys across a wide range of wavelengths are producing very large image databases of astronomical objects. For example, the Large Synoptic Sky Survey will produce billions of galaxy images.

Therefore, there is a need to build robust and automated tools for processing astronomical data, particularly for the analysis of the morphology of celestial objects such as galaxies. Galaxy classification is the first step towards a greater understanding of the origin and evolution process of the Universe, and to discover physical properties related to dark matter [33]. Edwin Hubble in 1926 devised a formal galaxy classification scheme, known as the Hubble tuning-fork [1]. This scheme grouped the galaxies based on their shape into three main types: elliptical, spiral and irregular. Elliptical galaxies have the shape of an ellipsoid. Spiral galaxies are divided into ordinary and barred: ordinary spirals have an approximately spherical nucleus, while barred spirals have an elongated nucleus that looks like a bar. Finally, irregular galaxies do not have an elliptical or spiral shape [1].

On one hand, visual inspection for classifying galaxies has been done traditionally by experts, but this time-consuming process requires several skills and high experience. On the other hand, automatic classification methods allow to analyze thousands of images in seconds, also these approaches are more objective and without of prejudices that probably are present in human methodology when looking at galaxy images [2].

Several approaches have been proposed for automatic image analysis and galaxy classification using machine learning and computer vision techniques. Many of this research work has been focused on artificial neural networks [2, 7, 17, 31], decision trees [24, 28], instance-based methods [30], kernel methods [16], among others. Recently, some interesting works have been introduced using new approaches. For example, the sparse representation technique and dictionary learning [11], rotation invariant descriptors [9], quaternion polar complex exponential transform moments [21], and deep neural networks [12, 25, 8, 22].

In this work, we hypothesized that *fractal dimension* quantification can be used in order to improve accuracy for classification of some types of galaxies and then justify their study in depth. Thus, we use the following methodology, composed by three stages, to perform galaxy classification: image processing; feature extraction using fractal dimension analysis and principal component; and classification using machine learning algorithms.

The paper is organized as follows. The next section provides a theoretical background on the fractal dimension analysis. Section 3 introduces the methodology for image-based galaxy classification. Section 4 describes experimental results and Section 5 presents a discussion. Finally, Section 6 outlines conclusions and directions for future work.

## 2 Fractal Dimension

Fractal dimension provides structural and spatial information of an object which could be a result of reaction or aggregation processes [23, 13, 3]. The *Haussdorf-Besicovich fractal dimension* (HB-fd) by box counting method [13, 19, 18, 20, 27] is a technique to provide information of the complexity of universe objects. It is necessary to use a spectrum of dimensional measures to characterize the total geometry for huge clusters of bright objects.

The fractal dimension formalism is based on the definition of the so-called multifractal spectra, this describes the evolution of the probability distribution of fractal structures. The analysis is performed on an image which is divided into small boxes until $\varepsilon_0$, then the probability of decomposition of the each box (i,Q) is calculated by:

$$P_{i,Q}(\varepsilon) = \frac{x_{i,Q}}{\sum x_{i,Q}} \propto \varepsilon^{\alpha}, \tag{1}$$

where $x_{i,Q}$ is the average height of shapes deposition inside the box of size $\varepsilon$, and $\alpha$ is the singularity of the subset of probabilities. It is suggested that the number of times that $\alpha$ in $P_{i,Q}$ takes a value between $\alpha'$ and $d\alpha'$, defined as $d\alpha'\rho(\alpha')\varepsilon^{-f(\alpha')}$ where $f(\alpha')$ is a continuous function. Then, the number of boxes of $\varepsilon$ with the same probability $P_{i,Q}(\varepsilon)$ is given by:

$$N_{\alpha}(\varepsilon) \propto \varepsilon^{f(\alpha)}, \tag{2}$$

where $f(\alpha)$ is the fractal dimension of the subset $\alpha$ [13, 19, 20, 27, 6]. After that, the probability $P_{i,Q}(\varepsilon)$ gives the rise of the partition function:

$$I(Q,\varepsilon) = \sum_{i=1}^{N(\varepsilon)} [P_{i,Q}(\varepsilon)]^{Q} = \varepsilon^{\tau(Q)}, \tag{3}$$

where $Q$ is the moment order. We used the scaling exponent defined by Halsey et al. [19, 18] where $\tau(Q)$ can take a width range of values measuring different regions of the set. The standard procedure [6] takes into account the generalized box-counting dimension defined as:

$$D_Q = \frac{1}{1-Q} \lim_{\varepsilon \to 0} \frac{lnI(Q,\varepsilon)}{ln(\varepsilon_0/\varepsilon)} = \frac{\tau(Q)}{Q-1}. \tag{4}$$

This spectrum generated by an infinite set of dimensions, measures the scaling structure as a function of the local pattern density. If *Q=0* the generalized fractal dimension represent the classic fractal dimension, i.e. $D_f = D_{Q=0}$. The exponent $\tau(Q)$ can be obtained from the slope of $lnI(Q,\varepsilon)$- $ln\varepsilon$ curve. Details of multi-fractal spectrum measures are described in [6, 5].

We select the case of $D_f = D_{Q=0}$ as the parameter of order in the images, where $\epsilon$ is the size of the box which acquire successively smaller values of length until the minimum value of $\epsilon_0$. Then, the probability to find is given by:

$$I(Q,\epsilon) = \sum_{i}^{N(\epsilon)} [P_{i,Q}]^{Q}, \tag{5}$$

where $Q$ is a parameter which gives the width of the spectrum and when $Q = 0$ the generalized fractal dimension represents the classical fractal dimension. In this work, the method was performed on gray scale images and using default sampling sizes. The distribution of particles at mesoscopic scales [35, 14, 10] or on macroscopic scales such as the famous fractality of the Britain island [23] were also taken into account for the parametrization.

## 3 Methodology for Galaxy Classification

The process to perform galaxy classification is divided into three main stages: 1) image processing, 2) feature extraction and 3) classification. In order to standardize the image data set, the images were rotated, centered and cropped, as we have already introduced in [7]. After that, features were extracted by calculating the fractal dimension, and principal component analysis. Finally, the numerical vectors were used as input parameters for the machine learning algorithms to classify the galaxies according to the main three types. Next subsections describe each stage in detail.

### 3.1 Image Processing

An image processing stage was performed to create a standardized image data set, which permits to extract some useful information from it. This process has been introduced in early work [7], therefore we only give a brief description.

The first step is to distinguish the galaxy contained in the image, then, a threshold is applied to obtain the pixels that form the galaxy: values greater than the threshold. Later, the images are rotated considering their main axis, which is given by the largest eigenvalue of the covariance matrix of the points in the galaxy image. Finally, the images are resized to 128x128 pixels. Figure 1 shows examples of original and standardized images for each type of galaxy.

### 3.2 Feature Extraction

Before performing classification, galaxy imagery must be represented as numerical vectors (features), which contain meaningful information. However, one of the main challenges when performing this task is to find the best method for characterizing the structural or geometrical properties of galaxies. In this study we have calculated the fractal dimension for each galaxy, which is considered as one of the attributes. Also, we used principal component analysis (PCA) to reduce the dimensionality of the images and to find a set of significant features.

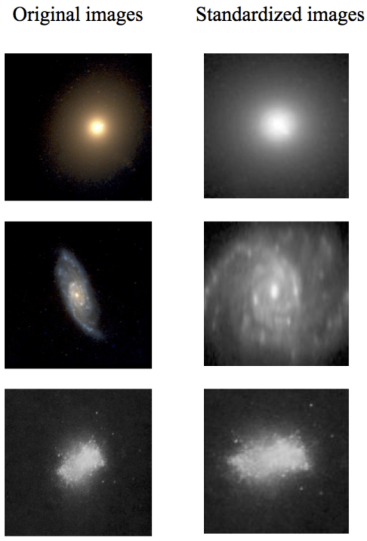


**Fig. 1.** Galaxy images used for experiments. Left: Original images, Right: Standardized images.

**Fractal Characterization.** The generalized fractal dimension was measured on different samples of the three main types of galaxies, following the procedure described in section 2.

Figure 2(a) presents the fractal dimension of 17 elliptical galaxies obtaining a fractal dimension value between $1.80 - 1.83$. The behavior of 104 spiral galaxies is presented in Figure 2(b), with values between $1.77 - 1.78$. Finally, Figure 2(c) shows the behavior of 10 irregular galaxies with values between $1.774 - 1.776$.

The ranks of the fractal dimension of these three types of galaxies are evidently different. The most of *HB-fd* of spiral galaxies are in a very similar range; irregular galaxies exhibit one dimension which correspond to structural properties of homogeneity[23]; while *HB-fd* on elliptical galaxies indicates structural wealth. The fractal dimension value for each galaxy was used as a parameter in the classification stage.

**Principal Component Analysis.** Principal component analysis (PCA) is a mathematical method that converts a (large) data set into a smaller number of variables called principal components (patterns). PCA, in machine learning, is an unsupervised method that reduces data while retaining meaningful patterns. These patterns are considered as a set of attributes that permit to differentiate the objects [32]. The first principal component accounts the largest variability in the data, and each subsequent component accounts the remaining

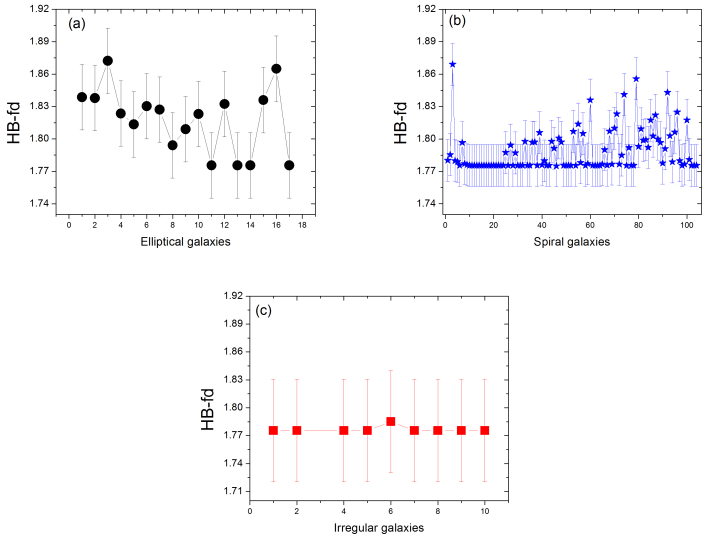


**Fig. 2.** In figure (a) black dots show the behavior of fractal dimension of elliptical galaxies. In figure (b) blue stars show the behavior of spiral galaxies. In figure (c) red squares presents the corresponding behavior related to irregular galaxies.

ones. This variability permits to rank the principal components according to their usefulness.

In our study, we have used 8 and 12 principal components, which represent about 80% of the information in original and standardized images, respectively; and 21 and 29 principal components, which represent about 90% of the information in the same way (see Figure 1 3). The projection of these principal components onto the original galaxy images were used as parameters for the classification stage.

### 3.3 Classification

For the classification stage we considered four representative algorithms of the supervised machine learning literature: a decision tree classifier (C4.5), an instance-based method (k-nearest neighbors), an ensemble classifier based on bootstrapping (random forest) and a linear discriminant (support vector machines).

Starting from a sample of labeled images, classification methods learn a function that aims to map unseen images to labels. In this study the labels are associated to the three main galaxy types of the Hubble sequence (i.e., elliptical, spiral or irregular). Before feeding images into classifiers, they must be represented as numerical vectors, thus, two representations were evaluated in this study: (i) The projection of images onto the first principal components, and (ii)

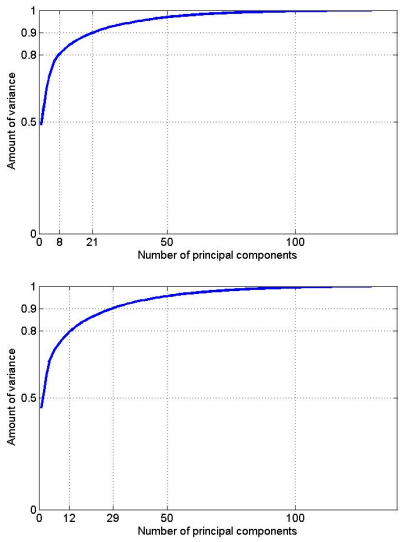


**Fig. 3.** Amount of cumulative variance of the principal components. Left: Original images. Right: Standardized images.

The same projection plus the *Haussdorf-Besicovich* fractal dimension (HB-fd) value, as an additional feature. Since the HB-fd is a physical measurement employed to describe structural properties of complex systems, our hypothesis is that including it in the representation of images will lead to better classification performance [23, 3]. The remainder of this section briefly describes the considered classification algorithms.

**C4.5.** It is an algorithm for learning decision tree classifiers [29]. Nodes of a decision tree are associated to thresholds on the attribute values in such a way that the tree induces a partition of the input space. Leaf nodes correspond to samples of the same class. When an unseen image has to be classified its associated vector representation is passed throughout the tree, the label corresponding to the leaf node reached by the feature vector is assigned to the image. The reader is referred to [29] for a more detailed explanation of this classifier.

**k-Nearest Neighbors.** The k-nearest neighbors (k-nn) classifier is an intuitive method that relies on similarities among instances to determine their class. k-nn memorizes a training set of labeled instances by storing them. When an unseen image needs to be classified, its feature vector is compared to the stored ones, then the k-most similar instances (the k-nn) are identified and used to determine the class of the image. Commonly the memory-based class of the nearest neighbors is assigned to a new instance. The similarity among instances

can be measured in many different ways, in this work we used the inverse of the Euclidean distance as similarity measure. An extensive treatment of k-nn is available in [26].

**Random Forest.** Random Forest (RF) is a committee or ensemble classifier formed by decision trees. Ensemble classifiers combine the outputs of many individual models trained for the same task, but that focus on different aspects of the problem. In the case of RF, decision trees are considered, each trained on a different subset of samples and dimensions of the feature vectors. When classifying a new instance, all of the individual models provide a prediction and RF returns the average output of the individual learners. RF, as other ensemble models, have theoretical bounds that guarantee the committee of learners outperforms individual models. Further information about RF can be found in [4].

**Support Vector Machines.** Support Vector Machines (SVMs) is a type of linear discriminant that guarantees obtaining the optimal hyperplane in the input-vector space that separates instances form two classes [34]. Linear discriminant aim at learning a linear function in the input space that separates examples of two classes. SVM finds such a function by maximizing the margin that separates instances from different classes. It provides a sparse solution as the decision function depends only in a subset of instances (the support vectors), which are the closest instances to the decision margin. SVM guarantees obtaining the optimal separating hyperplane in training data when the problem is linear separable. When linear separability does not hold, the *kernel trick* is used to map the original input space into another high-dimensional one where a linear function can separate the classes.

## 4 Experimental Results

The data set consisted of 131 images of galaxies: 17 elliptical, 104 spiral and 10 irregular; which were taken from different data bases of the web.

The experiments were carried out using Weka, a software package that implements machine learning algorithms for performing classification tasks [15]. We tested the following algorithms: decision trees, k-nearest neighbors, random forest and SVM. For the case of decision trees, and random forest we used default parameters. For the case of k-nn we used three neighbors with weighted distance, and we used a two-degree polynomial kernel for SVM.

In order to measure the overall accuracy of the machine learning algorithms, we used 10-fold cross-validation for all the experiments; that is, the original data set is randomly divided into ten equally sized subsets and performed 10 experiments, using in each experiment one of the subsets for testing and the other nine for training.

Tables 1 and 2 show the accuracy for each learning algorithm using the original images and the standardized ones, respectively. These results were

**Table 1.** Accuracy for original images using different number of principal components (PCs) and using the PCs plus the fractal dimension value (FDV). The best results are in bold.

| | PCs | | PCs + FDV | |
|---|---|---|---|---|
| Algorithm | 8 | 21 | 9 | 22 |
| C4.5 | 71.29 | 70.83 | 71.29 | 70.52 |
| 3-nn | 77.55 | **81.82** | 79.22 | **81.67** |
| RF | 78.31 | 80.91 | 80.30 | 80.60 |
| SVM | 79.38 | 79.53 | 79.38 | 79.99 |
| mean | 76.63 | 78.27 | 77.54 | 78.20 |

**Table 2.** Accuracy for standardized images using different number of principal components (PCs) and using the PCs plus the fractal dimension value (FDV). The best results are in bold.

| | PCs | | PCs + FDV | |
|---|---|---|---|---|
| Algorithm | 12 | 29 | 13 | 30 |
| C4.5 | 77.55 | 74.34 | 78.61 | 76.33 |
| 3-nn | 81.06 | 72.81 | 78.92 | 75.87 |
| RF | **85.95** | 85.33 | 85.94 | **86.71** |
| SVM | 79.84 | 73.27 | 85.49 | 83.20 |
| mean | 81.10 | 76.44 | 82.24 | 80.52 |

obtained by averaging the results of five runs of 10-fold cross-validation for each algorithm. On one hand, as we can observe from table 1, the best results were obtained by 3-nearest neighbors, with 81.82% accuracy using only PCs, and 81.67% accuracy using PCs plus the fractal dimension value. On the other hand, we can see from Table 2 that random forest obtained the best results with 85.95% and 86.71% accuracy, using PCs and PCs plus the fractal dimension value, respectively.

Tables 3 and 4 present the accuracy of the algorithms using only one feature, that is, 1 principal component (1-PC) and the fractal dimension value. Also, we show the results using 1-PC plus the fractal dimension value. From these tables, we can observe that random forest obtained five of the best results, while C4.5 obtained the other one. In addition, we can see that, on average, classification using the fractal dimension value is better than using 1-PC, considering standardized images.

## 5 Discussion

Figure 4 presents a summarizing of the *HB-fd* values for the three types of galaxies. As we can observe from this Figure, the characterization by fractal dimension helps to distinguish the type of galaxy.

Results presented in Tables 1 and 2 show that the best results are obtained when standardized images and fractal dimension are used, particularly using random forest with 29 PCs plus the fractal dimension value. In addition, it

**Table 3.** Accuracy for original images using 1 principal component (1 PC) and the fractal dimension value (FDV). The best results are in bold.

| Algorithm | 1 PC | FDV | 1 PC + FDV |
|---|---|---|---|
| C4.5 | **79.68** | 77.09 | **79.38** |
| 3-nn | 76.02 | 70.22 | 74.04 |
| RF | 74.34 | 65.79 | 74.34 |
| SVM | 79.38 | **79.38** | **79.38** |
| mean | 77.35 | 73.12 | 76.78 |

**Table 4.** Accuracy for standardized images using 1 principal component (1 PC) and the fractal dimension value (FDV). The best results are in bold.

| Algorithm | 1 PC | FDV | 1 PC + FDV |
|---|---|---|---|
| C4.5 | 78.92 | 78.46 | 75.56 |
| 3-nn | 74.49 | 78.16 | 77.24 |
| RF | 68.39 | 75.11 | 76.17 |
| SVM | **79.38** | **79.22** | **78.62** |
| mean | 75.29 | 77.74 | 76.90 |

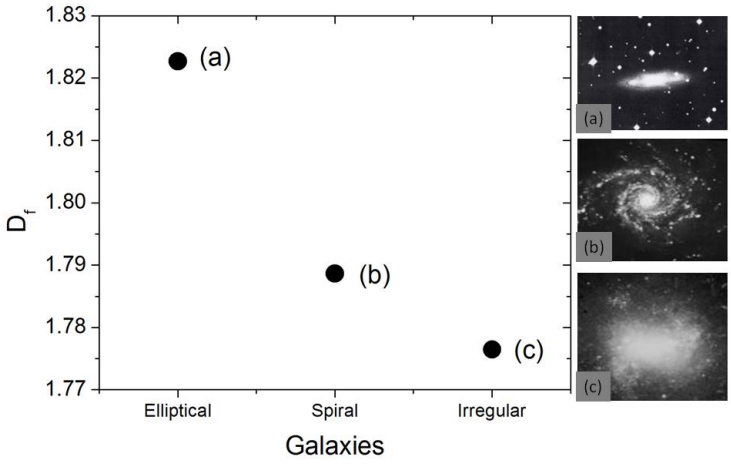


**Fig. 4.** Fractal dimension for three galaxies: (a) shows an example of an elliptical galaxy with fractal dimension value of $HB - fd = 1.8226$; (b) shows an image of an spiral galaxy, its fractal dimension value is $HB - fd = 1.7886$; finally, (c) presents an example of an irregular galaxy with a value of $HB - fd = 1.7764$.

can be observed that SVM was the algorithm with the largest improvement of accuracy when using PCs plus the fractal dimension value. Specifically, a better evaluation (from 73.27% to 85.29%) is obtained by using 29 and 30 features.

**Table 5.** Confusion matrix for the best algorithm to classify elliptical galaxies: 3-nearest neighbors.

| Galaxy type | Elliptical | Spiral | Irregular | Accuracy per type |
|---|---|---|---|---|
| Elliptical | 15 | 2 | 0 | 88.9 % |
| Spiral | 12 | 92 | 0 | 88.4 % |
| Irregular | 1 | 9 | 0 | 0 % |

**Table 6.** Confusion matrix for the best algorithm to classify spiral galaxies: Random forest.

| Galaxy type | Elliptical | Spiral | Irregular | Accuracy per type |
|---|---|---|---|---|
| Elliptical | 11 | 6 | 0 | 64.7 % |
| Spiral | 0 | 104 | 0 | 100.0 % |
| Irregular | 0 | 10 | 0 | 0 % |

**Table 7.** Confusion matrix for the best algorithm to classify irregular galaxies: C4.5.

| Galaxy type | Elliptical | Spiral | Irregular | Accuracy per type |
|---|---|---|---|---|
| Elliptical | 9 | 8 | 0 | 52.9 % |
| Spiral | 8 | 91 | 5 | 87.5 % |
| Irregular | 2 | 4 | 4 | 40.0 % |

In fact, in average among the different classifiers, the performance classification improved by more than 4% when including the fractal dimension value as a feature.

In Tables 5, 6 and 7 we present the confusion matrix for the best result obtained to classify elliptical, spiral and irregular galaxies, respectively. From these results we can see that 3-nearest neighbors was the best algorithm to classify elliptical galaxies with 88.9% accuracy; random forest was able to classify with 100% accuracy of the spiral galaxies; while C4.5 was the best algorithm to classify irregular galaxies with 40% accuracy. We can also observe that none of the best results for elliptical and spiral galaxies have classified irregular galaxies correctly. On the other hand, when irregular galaxies are classified correctly, the accuracy of elliptical decreases significantly; while the accuracy for spiral galaxies remains about 87% accuracy.

## 6 Conclusions

In this paper we have introduced the fractal dimension analysis to perform image-based galaxy classification. The fractal dimension value contributes to improve the classification accuracy for the three main types of galaxies, despite using a small data set of images for training the classifiers. The best results were obtained by 3-nearest neighbors and random forest using standardized images with PCs and the fractal dimension value. Directions for future work includes to identify more types of galaxies and testing some approaches of deep learning with fractal dimension analysis.

## References


1. Ball, N.: Morphological Classification of Galaxies Using Artificial Neural Networks. Master's thesis, University of Sussex (2002)
2. Ball, N., Loveday, J., Fukugita, M., Nakamura, O., Okamura, S., Brinkmann, J., Brunner, R. J.: Galaxy types in the sloan digital sky survey using supervised artificial neural networks. Monthly Notices of the Royal Astronomical Society, vol. 348, pp. 1038–1046 (2004)
3. Barnsley, M.: Fractals everywhere. Dover publications (2012)
4. Breiman, L.: Random forests. Machine Learning, vol. 45, pp. 5–32 (2001)
5. De la Calleja, E., Bazoni, R., Rocha, M., Barbosa, M.: Topology of dna: a honeycomb stable structure under salt effect. arxiv.org/abs/1706.02685, (2018)
6. De la Calleja, E., Cervantes, F., De la Calleja, J.: Order-fractal transitions in abstract paintings. Annals of Physics, vol. 371, pp. 313–322 (2016)
7. De la Calleja, J., Fuentes, O.: Machine learning and image analysis for morphological galaxy classification. Monthly Notices of the Royal Astronomical Society, vol. 349, pp. 87–93 (2004)
8. Cavanagh, M. K., Bekki, K.: Bars formed in galaxy merging and their classification with deep learning. Astronomy and Astrophysics, vol. 641 (2020)
9. Cecotti, H.: Rotation invariant descriptors for galaxy morphological classification. International Journal of Machine Learning and Cybernetics, vol. 11, pp. 1839–1853 (2020)
10. Chhabra, A., Meneveau, C., Jensen, R., Sreenivasan, K.: Direct determination of the f($\alpha$) singularity spectrum and its application to fully developed turbulence. Phys. Rev. A, vol. 40, pp. 5284 (1989)
11. Diaz-Hernandez, R., Ortiz-Esquivel, A., Peregrina-Barreto, H., Altamirano-Robles, L., Gonzalez-Bernal, J.: Automatic approach to solve the morphological galaxy classification problem using the sparse representation technique and dictionary learning. Experimental Astronomy, vol. 41, pp. 409–426 (2016)
12. Dieleman, S., Willett, K., Dambre, J.: Rotation-invariant convolutional neural networks for galaxy morphology prediction. Monthly Notices of the Royal Astronomical Society, vol. 450, pp. 1441–1459 (2015)
13. Feigenbaum, M., Jensen, M., Procaccia, I.: Time ordering and the thermodynamics of strange sets: Theory and experimental tests. Phys. Rev. Lett., vol. 57, pp. 1503 (1986)
14. Ferreira, T., Rasband, W.: Imagej user guide. http::/rsb.info.nih.gov/ij/docs/guide/user-guide.pdf (2013)
15. Frank, E., Hall, M., Witten, I.: The WEKA Workbench. Online Appendix for Data Mining: Practical Machine Learning Tools and Techniques. Morgan Kaufmann (2016)
16. Freed, M., Lee, J.: Krylov iterative methods for support vector machines to classify galaxy morphologies. Journal of Data Analysis and Information Processing, vol. 03, pp. 72–86 (2015)
17. Goderya, S., Lolling, S.: Morphological classification of galaxies using computer vision and artificial neural networks: A computational scheme. Astrophysics and Space Science, vol. 279, pp. 377–387 (2002)
18. Halsey, T., Jensen, M., Kadanoff, L., Procaccia, I., Shraiman, B.: Erratum: Fractal measures and their singularities: The characterization of strange sets. Physical Review A, vol. 34, pp. 1601 (1986)

19. Halsey, T., Jensen, M., Kadanoff, L., Procaccia, I., Shraiman, N.: Fractal measures and their singularities: The characterization of strange sets. Phys. Rev. A, vol. 33, pp. 1141 (1986)
20. Hentschel, G., Procaccia, I.: The infinite number of generalized dimensions of fractals and strange attractors. Physica D, vol. 8, pp. 435–444 (1983)
21. Hosny, K., Elaziz, M., Selim, I., Darwish, M.: Classification of galaxy color images using quaternion polar complex exponential transform and binary stochastic fractal search. Astronomy and Computing, vol. 31, pp. 1–13 (2020)
22. Lalit, M. G., Maanak, A., Tushar, P., Mamta, M.: Morphological classification of galaxies using conv-nets. Earth Science Informatics, vol. 13, pp. 1427–1436 (2020)
23. Mandelbrot, B.: How long is the coast of britain? statistical self-similarity and fractional dimension. Science, vol. 156, pp. 636–638 (1967)
24. Marin, M., Sucar, L., Gonzalez, J., Diaz, R.: A hierarchical model for morphological galaxy classification. FLAIRS Conference, (2013)
25. Misra, D., Mohanty, S. N., Agarwal, M., Gupta, S. K.: Convoluted cosmos: Classifying galaxy images using deep learning. Data Management, Analytics and Innovation, vol. 1, pp. 569–579 (2020)
26. Mitchell, T.: Machine learning. McGrawHill (1997)
27. Ott, E.: Chaos in Dynamical Systems. Cambridge University Press, United States of America (1993)
28. Owens, E., Griffiths, R., Ratnatunga, K.: Using oblique decision trees for the morphological classification of galaxies. Monthly Notices of the Royal Astronomical Society, vol. 281, pp. 153–157 (1996)
29. Quinlan, J.: Induction of decision trees. Machine Learning, vol. 1, pp. 81–106 (1986)
30. Shamir, L.: Automatic morphological classification of galaxy images. Monthly Notices of the Royal Astronomical Society, vol. 399, pp. 1367–1372 (2009)
31. Sodré, L., Storrie-Lombardi, M., Lahav, O., Storrie-Lombardi, L.: Morphological classification of galaxies by artificial neural networks. Monthly Notices of the Royal Astronomical Society, vol. 259, pp. 8–12 (1992)
32. Turk, M., Pentland, A.: Face recognition using eigenfaces. In: IEEE Conference on Computer Vision and Pattern Recognition., pp. 586–591 (1991)
33. Van Dokkum, P., Danieli, S., Cohen, Y., Merritt, A., Romanowsky, A., Abraham, R., Brodie, J., Conroy, C., Lokhorst, D., Mowla, L., E., O., Zhang, J.: A galaxy lacking dark matter. Nature, vol. 555, pp. 629–632 (2018)
34. Vapnik, V.: The nature of statistical learning theory. Springer (1995)
35. Weitz, D., Oliveria, M.: Fractal structures formed by kinetic aggregation of aqueous gold colloids. Phys. Rev. Lett, vol. 52, pp. 313–322 (1984)